Determination of protein synthesis on a proteomic scale

Kramer, G.

Publication date
2011

2

Effects of azidohomoalanine on bacterial growth, viability and protein function

Summary

The methionine analogue azhal has been used to identify newly synthesized proteins in mammalian cells. The azide group of azhal can be used to specifically enrich labelled proteins, enabling short labelling times. However, not much is known regarding the effects of azhal on cellular physiology and protein function. The suitability of azhal-labelling was tested for two prokaryotic model organisms. Growth in the presence of the analogue was analyzed for methionine-auxotrophic strains of *E. coli* and *B. subtilis*. *E. coli* grows equally well on azhal as on methionine during the first 30 minutes, then gradually growth arrest sets in. Viability and cellular protein content were similar as well, and azhal showed no direct toxicity. In contrast, *B. subtilis* grown on the analogue displayed an initial lag phase and a much lower growth rate. In addition, azhal was toxic at higher concentrations. Nonetheless, *B. subtilis* did also incorporate azhal into proteins.

The effects of azhal on protein structure and function were investigated by producing recombinant proteins in the presence of azhal. Three photo-active proteins: PYP, YtvA and AppA had all their methionine residues replaced by azhal. This shows *E. coli* readily incorporates the analogue into proteins. For all three proteins the UV-VIS spectra were identical to those of their non-labelled counterparts, strongly indicative of correct folding. Recovery from signalling to ground state, after illumination, was slower for azPYP and azYtvA but faster for azAppA compared to the methionine containing proteins. In contrast, recombinant LacZ could not be detected upon induction in the presence of azhal. The initial unperturbed growth on azhal in *E. coli* and the lack of major changes in structure and stability of the three photo-active proteins studied, makes azhal pulse-labelling an excellent tool to determine cellular translation rates.

Introduction

The use of radiolabelled amino acids to determine synthesis and degradation-rates through pulse-chase labelling is a technique which has been used throughout biochemical and physiological research as outlined in *Chapter 1*. Recently however, in efforts to identify and quantitate newly synthesized proteins, the use of non-natural amino acids have emerged as an alternative (141, 167-169). Most notable amongst these non-natural amino acids is the methionine analogue azhal. This methionine analogue was first reported to increase mutational rates in *Salmonella typhimurium* (174), but incorporation into proteins was not studied. Azhal is efficiently incorporated into proteins by both *E. coli*, mammalian and insect cells grown in its presence (141, 143, 144, 148, 169, 171), even though the k_{cat}/K_m of *E. coli* methionyl-tRNA-synthetase for azhal is 390 times lower than for methionine (144). The azide group of azhal makes it amenable to derivatization using different chemistries, facilitating both fluorescent tagging of azhal labelled proteins as well as enhanced mass spectrometric detection of these proteins with different enrichment schemes (see *Chapter 1*). As such, azhal seems a promising label to probe protein synthesis- and degradation-rates on a proteome-wide scale.

However, the suitability of azhal as a pulse-label does not depend solely on its incorporation into (recombinant)-proteins but also on its ability to reflect protein synthesis during pulse-labelling. This is governed by azhal's direct and indirect effects on cellular physiology, through toxicity and relative functionality of azhal-containing proteins. Knowledge about the effects of azhal on cellular physiology is limited, apart from the mutagenicity study in *S. typhimurium* mentioned above, but mammalian cells have been reported to be viable up to two hours after pulse-labelling with azhal as determined by a dye exclusion assay (168). There is somewhat more evidence about how azhal affects the proteins containing it. Display of OmpC at the cell surface of *E. coli* (148, 150) suggests normal folding of azhal-containing proteins as does a study which showed that viral envelope proteins containing azhal assemble into a viral envelope structure (151). A study by Wang *et al.* showed that a recombinant protein containing azhal undergoes N-terminal processing (175) and Dieterich *et al.* did not find large differences in degradation-rates of azhal-containing proteins compared to their unlabelled counterparts in mammalian cells (168). The only report regarding effects of azhal incorporation on specific enzyme activity is on lipase B from *Candida antartica* expressed in an auxotrophic *E. coli*, grown in the presence of azhal, which was found to be 75% that of the methionine containing enzyme (176). Until now azhal has only been applied as a pulse-label in *E. coli,* mammalian and insect cells, (141, 168, 169, 171). So investigating the wider application of azhal in different organisms is important.

Here we report on the potential usefulness of azhal as a pulse-label in two prokaryotic model organisms, i.e. the Gram-negative bacterium *E. coli* and Gram-positive bacterium *B. subtilis*. We measured growth of the bacteria in the presence of azhal to determine the time-frame in which azhal-labelling could give an accurate indication of protein synthesis-rate without interfering with cellular physiology. In addition, effects of incorporation of azhal on protein structure, function and stability were studied with recombinant proteins. We studied three photo-active proteins, i.e. photo-active yellow protein (His-tagged PYP, 15.8 kD, 6 methionines, monomer) from *Halorhodospira halophila* (177), the antirepressor of ppsR, sensor of blue light (AppA His-tagged BLUF-domain, 15.4 kD, 5 methionines, dimer) from *Rhodobacter sphaeroïdes* (178) and the blue-light photoreceptor (His-tagged YtvA, 30.5 kD, 8 methionines, dimer) from *B. subtilis* (179) in addition we tested β-galactosidase (LacZ, 116 kD, 23 methionines, tetramer) from *E. coli*. The photo-active proteins undergo conformational changes upon illumination with light and go through a photocycle (Figure 1) that can be studied by UV-VIS spectroscopy to find possible changes induced by azhal incorporation. For measuring β-galactosidase activity a colorimetric assay was used.

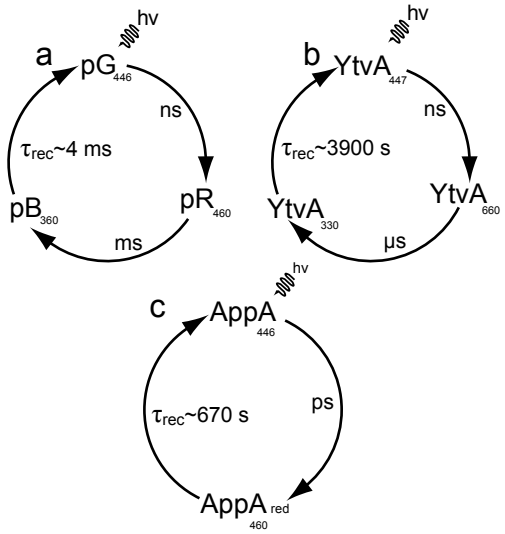

FIGURE 1. **Photocycles of PYP, YtvA and AppA.** Basic photocycle of PYP showing the ground state pG (P or PYP) and key intermediates pR (I_1 or PYP_L) and pB (I_2, PYP_M) formed upon illumination of the protein with photoflash light (**a**). pB is PYP's signalling state in which the chromophore (coumaric acid) has been protonated and the protein structure has changed. The absorbance maxima for the intermediates are shown, the time-scales for the conversion from pG to pR and pR to pB are given, as well as the mean lifetime of the recovery from pB to pG (189) which was measured in the current study to see effects of azhal incorporation on the photocycle. Photocycle of YtvA, showing the ground state ($YtvA_{447}$) and the time-scale upon which intermediates $YtvA_{660}$ and signalling state $YtvA_{330}$ are formed upon illumination (**b**). The mean recovery time from $YtvA_{330}$ to $YtvA_{447}$ is given, numbers denote the absorbance maxima of different intermediates and ground state (209, 210). AppA's photocycle is shown (**c**) with the ground state (AppA) and the red-shifted signalling state ($AppA_{red}$) with their absorbance maxima and mean lifetime of the recovery to the ground state (200, 211, 212).

RESULTS

Growth rate and viability of E. coli cultured on azhal— E. coli has previously been shown to efficiently incorporate azhal into recombinant proteins (143-151). However, for pulse-labelling applications under relevant physiological conditions, it is important to know how *E. coli* grows on azhal and incorporates it into cellular proteins. The K_{cat}/K_m of methionyl-tRNA-synthetase for azhal is 390 times lower than for methionine (144). No residual methionine should thus be present during labelling to ensure maximum efficiency of label incorporation. Therefore a methionine-auxotrophic *E. coli* strain is needed for growth experiments. The methionine auxotroph MTD123 (180) was selected to ensure that no residual methionine was present, cells were harvested and washed prior to addition of azhal as described in *experimental procedures*. A range of azhal-concentrations, from 10 mg/l to 1000 mg/l was tested. Both the growth rate (Figure 2a) and the growth yield (data not shown) are maximal at azhal concentrations of 250 mg/l and higher. For further experiments an azhal concentration of 400 mg/l was chosen.

When *E. coli* cells are growing rapidly, incorporation of radiolabelled compounds into proteins is closely related to growth rate (38). Thus, the degree of azhal-labelling can

be estimated by the increase in cell number as measured by optical density. For the first 30 minutes after inoculation cells grow with similar doubling times for azhal and methionine (Figure 2b). In addition, the amount of cellular protein per OD_{600} is also similar for cells grown on azhal (Figure 3a). After 30 minutes there is a marked decrease in growth rate of the cells growing on azhal. These cells, after having completed more than one doubling at the reduced growth rate, gradually enter stationary phase after more than five hours. Similar results were obtained with the auxotrophic strains CAG18941 and M15MA. This demonstrates that growth rate and increase in protein content in the presence of azhal is similar to that of cells grown on methionine, but only for the first 30 minutes upon incubation of cells with the methionine analogue.

To investigate if cells are still viable after labelling with azhal, samples were taken during growth. Up to 30 minutes, the number of viable cells per unit of OD_{600} remains constant between cells grown on azhal and methionine (Figure 3b). The number of viable cells grown on azhal decreased after one hour of labelling. Toxic effects not related to incorporation of azhal into proteins were tested by growing cells on a mix of azhal and methionine. Because of the lower efficiency of charging azhal to tRNA by the methionyl-tRNA-synthetase,

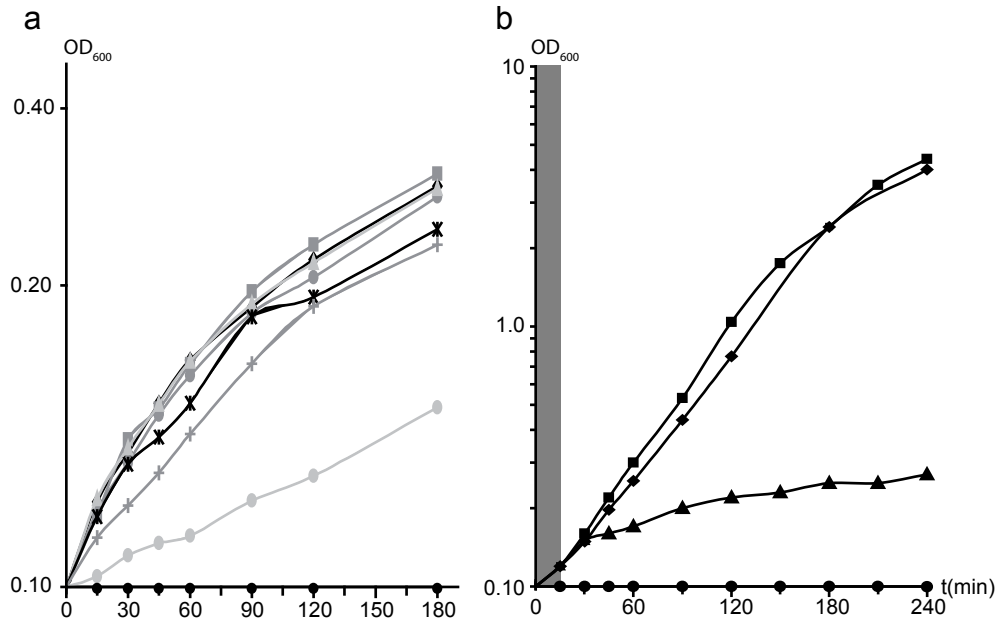

FIGURE 2. **Growth of *E. coli* on different concentrations of azhal**. Growth of *E. coli* strain MTD123 on 10 mg/l azhal (light grey circles), 50 mg/l azhal (dark grey crosses), 100 mg/l azhal (black crosses), 250 mg/l azhal (light grey triangles), 400 mg/l azhal (dark grey squares), 500 mg/l azhal (dark grey circles), 1000 mg/l (black diamonds) or control (black circles) (**a**). No alteration in growth rate is observed above 250 mg/l of Azhal. Growth curve of *E. coli* strain MTD123 on minimal medium containing either 60 mg/l Methionine (squares), 400 mg/l azhal (triangles), a mix of 60 mg/l methionine and 400 mg/l azhal (diamonds) or neither as a negative control (circles) (**b**). Growth rate on methionine alone is 1.15 h^{-1} ± 0.04. Growth rate on azhal plus methionine is 1.11 h^{-1} ± 0.03. The grey box shows the time frame envisioned for pulse-labelling cells with azhal.

incorporation into proteins is negligible under these conditions. Growth rate was compared with cells grown on methionine alone and is similar (Figure 2b). No effects of azhal not incorporated into proteins on cellular physiology are apparent from this experiment.

As an alternative for batch cultures combined with washing to remove excess of methionine prior to azhal-labelling, methionine limited continuous cultures can be used. These enable extremely short pulse-labelling times, since large cultures at high cell densities can be employed, while possible washing-related stresses are avoided. For such a future application we tested strains in methionine limited chemostat culture. We found CAG19491 and M15MA to be unstable auxotrophes in continuous culture. These strains regained the ability to produce methionine endogenously within 24-48 hours of continuous culturing. Although both strains perform well in batch experiments and in producing azhal-labelled recombinant proteins (see below), only MTD123 was used for further labelling experiments.

The work described thus far has been carried out with the MTD123 strain, but growth characteristics of the wild type *E. coli* K12 strain suggests that application of azhal pulse-labelling does not have to be confined to auxotrophes. When grown in minimal medium containing methionine and shifted to minimal medium without methionine, *E. coli* K12 cells show a lag phase of ~15-30 minutes before resuming growth (Figure 4a and b). This is due to the time needed to turn on the methionine bio-synthesis pathway and generate enough endogenous methionine for growth. In contrast, wild type cells shifted to minimal medium containing azhal resume growth immediately at the same rate as the auxotrophic strain for the first 30 minutes (Figure 4b). After 30 minutes the growth of *E. coli* K12 grown on azhal also starts to slow, however, presumably because endogenous methionine biosynthesis is switched on, it recovers growth rate (Figure 4a). This is in accordance with the results obtained for

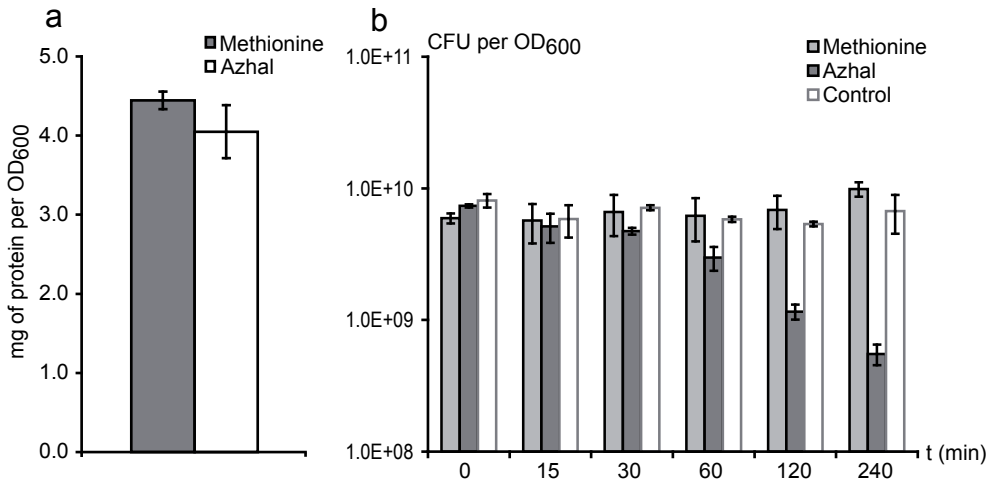

FIGURE 3. **Viability and protein content of *E. coli* grown on azhal**. The amount of total cellular protein per OD_{600} of cells grown on azhal or methionine for the first 30 minutes of growth (**a**). Number of colony forming units per OD_{600} per ml of culture over time. MTD123 cells grown on 60 mg/l methionine or 400 mg/l azhal compared to cells that are in stationary phase in minimal medium without methionine or azhal (**b**).

the auxotroph cultured on a mix of methionine and azhal (Figure 2b). This suggests that wild type *E. coli* strains can be employed as well, provided that labelling times with azhal are short enough to prevent incorporation of methionine in newly synthesized proteins in the course of the pulse. However, we chose to continue the use of the auxotrophic strain to preclude any endogenous methionine biosynthesis interfering with azhal-labelling.

In the experiments described in the previous paragraphs, we have shown that methionine-auxotrophic *E. coli* strains grew at a normal rate for 30 minutes on azhal as a methionine analogue in M9 minimal medium supplemented with all 19 other natural amino acids. These experiments pave the way to use azhal in pulse-labelling experiments in order to identify and quantify proteins synthesized in a short time frame upon an environmental perturbation. Most often stable-isotopes are used for relative quantitation by mass spectrometry. Several methods have been described, either using *in vivo* (181, 182) or *in vitro* (25, 183-186) labelling. *In vivo* labelling has the advantage that pulse-labelling with azhal and introduction of the stable-isotopes occur simultaneously. One possibility for *in vivo* labelling would be application of heavy and light variants of azhal. However, the heavy variant would require expensive ^{13}C- and/or ^{15}N- labelled precursors for its synthesis. Another possibility would be metabolic labelling with stable-isotopes by using a ^{13}C carbon or ^{15}N nitrogen source in the minimal growth medium in one condition and the ^{12}C and ^{14}N counterparts

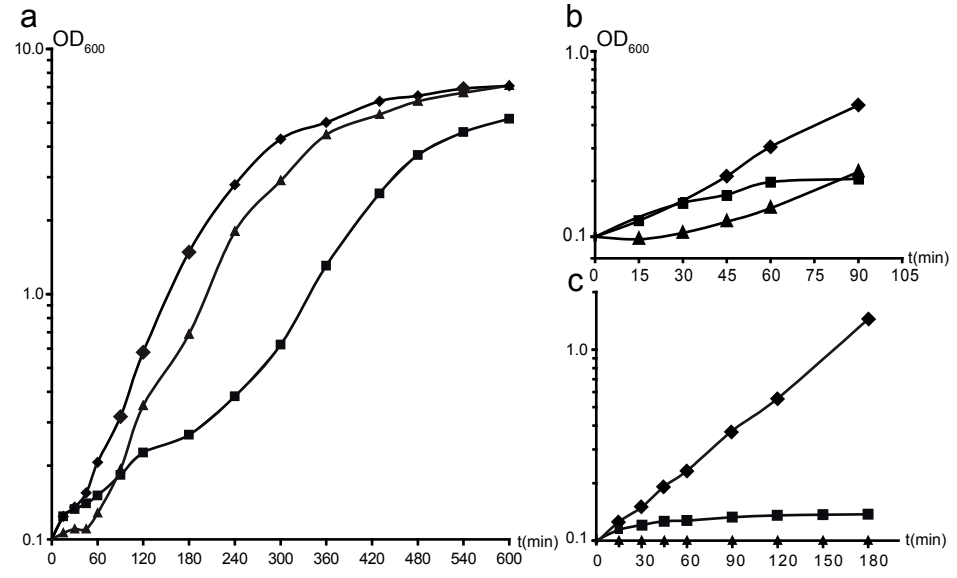

FIGURE 4. **Growth of wild type *E. coli* on azhal and growth of auxotrophic *E. coli* in medium without amino acids in the presence of azhal**. Long term growth of wild type *E. coli* strain K12 on minimal medium containing 60 mg/l methionine (diamonds), 400 mg/l azhal (squares) or neither as a negative control (triangles) (**a**). The initial 90 minutes of the curve shown in (a), shows that growth rate on azhal is similar to growth on methionine for the first 30 minutes, while the negative control resumes growth after a lag phase of about 15-30 minutes (**b**). Growth of the methionine-auxotrophic strain MTD123 on minimal medium not supplemented with 19 amino acids (i.e. all except methionine), containing either methionine, azhal or neither as a negative control (**c**), symbols as in panel (**a**).

in the other. In the experiments with azhal described thus far, *E. coli* was cultured on M9 minimal medium supplemented with 19 amino acids. However, the presence of amino acids in the medium hampers labelling of proteins with stable-isotopes, unless very expensive ^{13}C- or ^{15}N-labelled amino acids are applied. So, to investigate if metabolic labelling could be used to quantify azhal-labelled proteins, MTD123 was grown on M9 minimal medium without addition of the 19 amino acids but containing methionine. Following washing as described in the *experimental procedures* section, cells were transferred to M9 minimal medium containing 400 mg/l azhal without amino acids and OD_{600} was recorded (Figure 4c). Although growth on azhal initially is still similar to growth on methionine, it is only so for 15 minutes following inoculation (Figure 4c). After that, cells cultured on azhal stop growing and enter stationary phase. This shows that addition of amino acids to the medium attenuates azhal-induced growth arrest and indicates that metabolic labelling with ^{13}C and or ^{15}N-labelled amino acid precursors as a quantitative approach is not useful in conjunction with azhal pulse-labelling. Why the addition of amino acids attenuates growth arrest is not entirely clear. Since *in vivo* labelling to introduce heavy and light stable-isotopes turned out to be unpractical in combination with the use of azhal as a pulse-label, we choose application of an *in vitro* method, i.e. the use of iTRAQ (isobaric tagging reagents for relative and absolute quantitation) (183) to quantify newly synthesized proteins (i.e., azhal-labelled proteins) in the experiments described in the following chapters.

B. subtilis grows on azhal and incorporates it into cellular proteins— The Gram-negative model organism, *E. coli,* grows normally on azhal for the initial 30 minutes. Next, Gram-

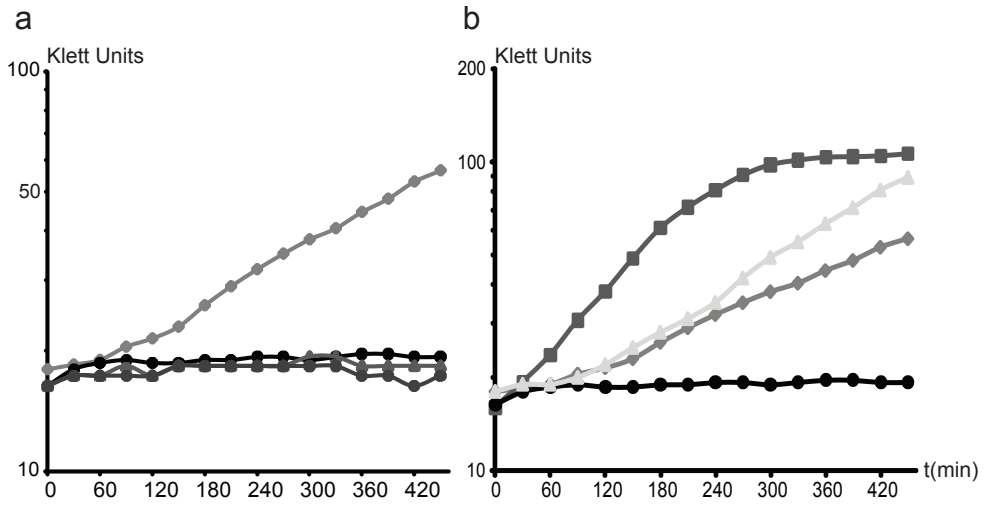

FIGURE 5. **Growth of the methionine-auxotrophic *B. subtilis* strain BR151:*yitJ-lacZ* grown in the presence of azhal**. Growth of *B. subtilis* in the presence of 200 mg/l azhal (grey diamonds), 800 mg/l azhal (grey triangles) or 2000 mg/l azhal (grey circles). Black circles, control (**a**). Growth of *B. subtilis* in minimal medium containing either 50 mg/l methionine (grey squares), 200 mg/l azhal (grey diamonds), a mix of 50 mg/l methionine/200 mg/l azhal (grey triangles) or neither, as a negative control (black circles) (**b**).

positive *B. subtilis* was used to see whether this organism also able to grow on azhal and incorporate it. The methionine-auxotrophic strain BR151 (*yitJ:lacZ)* was cultured in Spizizen minimal medium containing methionine, and after washing was transferred to medium containing azhal. Surprisingly, *B. subtilis* does not grow at all on azhal at concentrations of 0.8 g/l or 2 g/l. (Figure 5a) suggesting a direct dose dependent toxic effect of azhal. Cells grown on 200 mg/l of azhal go into lag-phase for about an hour before resuming growth whereas cells grown on methionine resume growth immediately (Figure 5b, $t_{doubling}$ 1.5 hours). After the lag-phase cells with azhal in the medium resume growth at a lower rate ($t_{doubling}$ 3.75 hours) but continue to grow for over six hours without any sign of going into lag phase. When *B. subtilis* was grown on a mix of azhal and methionine, the initial lag phase remained. Although growth rate did increase ($t_{doubling}$ 2.5 hours) it did clearly not increase to the growth rate of cells grown on methionine alone. This suggests either competition between azhal and methionine for charging to the methionyl-tRNA-synthetase, which is unlikely given the results for growth on different concentrations of azhal, or a direct toxic effect of azhal which is independent of its incorporation into proteins, consistent with its dose dependent cytostatic effect. Nevertheless, growth of this auxotrophic strain on azhal suggests azhal is incorporated into cellular proteins. This indeed proved to be the case (see below).

The *Bacillus* strain used also contained a *yitJ:lacZ* fusion. YitJ is a homocysteine s-methyltransferase and catalyzes one of the steps in the bio-synthesis of methionine in *B. subtilis*. Using the fusion with LacZ, the activation of methionine biosynthesis in response

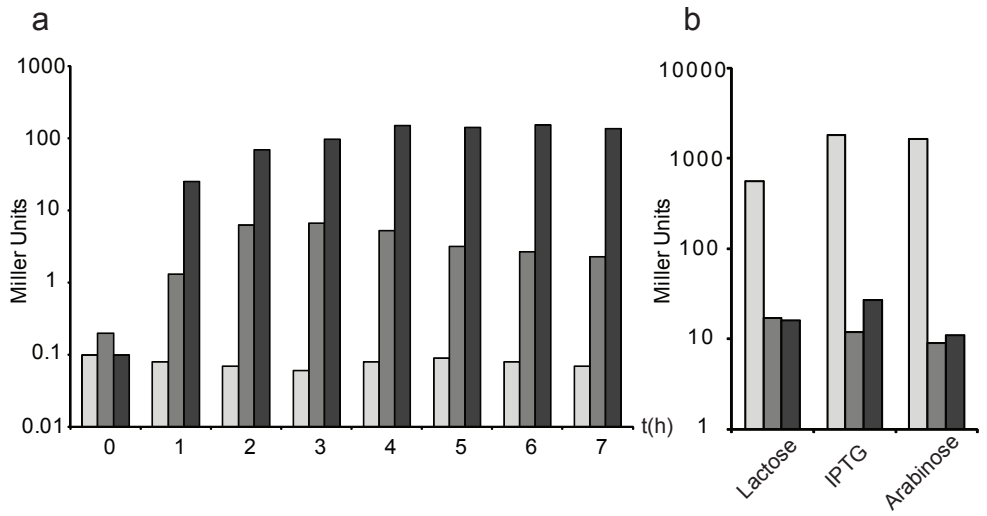

FIGURE 6. **Induction of methionine biosynthesis in *B. subtilis* and** LacZ **activity in *E. coli* grown in the presence of azhal.** LacZ activity as a measure of the induction of the methionine biosynthesis route measured in *B. subtilis* methionine-auxotrophic strain BR151:*yitJ:lacZ* grown in minimal medium containing methionine (light grey bars), azhal (dark grey bars) or neither (black bars) (**a**). LacZ activity measured 3 hours after induction of *E. coli* strain CAG18491/LacZ with lactose, IPTG or arabinose in minimal medium containing methionine (light grey bars), azhal (dark grey bars) or neither (black bars) (**b**).

to methionine starvation can be measured. Figure 6a shows that in a methionine containing medium YitJ expression is repressed, while it is induced in the absence of methionine. Nevertheless cells cannot grow in a methionine-deprived medium due to a mutation in *metB,* encoding a putative homoserine o-acetyltransferase, which blocks the homocysteine biosynthesis pathway. There is also induction of *yitJ* in methionine-deprived cells in the

TABLE I
Azhal containing proteins identified in B. subtilis

No.	Acc. No.	Description	Score†	No. Matches
1	Q04747	Surfactin synthetase subunit 2	1532	35
2	P33166	Elongation factor Tu	1205	22
3	P26901	Vegetative catalase	609	15
4	P27206	Surfactin synthetase subunit 1	527	11
5	Q9KWU4	Pyruvate carboxylase	423	10
6	P28598	60 kDa chaperonin	664	9
7	P02968	Flagellin	465	9
8	P80866	Vegetative protein 296	280	9
9	P37527	Pyridoxal biosynthesis lyase pdxS	358	7
10	O32162	YurU protein	230	7
11	Q08787	Surfactin synthetase subunit 3	453	6
12	P80700	Elongation factor Ts	185	6
13	P49814	Malate dehydrogenase	368	5
14	P21879	Inosine-5'-monophosphate dehydrogenase	216	5
15	P42318	Uncharacterized protein yxjG	212	5
16	P37809	ATP synthase subunit beta	169	5
17	P19669	Transaldolase	139	5
18	P45740	Thiamine biosynthesis protein thiC	268	4
19	P39120	Citrate synthase 2	218	4
20	P09124	Glyceraldehyde-3-phosphate dehydrogenase 1	203	4
21	P37571	Neg. regul. of genetic competence clpC/mecB	162	4
22	P80865	Succinyl-CoA ligase subunit alpha	147	4
23	P40780	Uncharacterized protein ytxH	230	3
24	P21880	Dihydrolipoyl dehydrogenase	206	3
25	P42974	NADH dehydrogenase	139	3
26	O32156	Unchar. ABC transp. Extracell.-bind. protein yur	131	3
27	P39644	Bacilysin biosynthesis oxidoreductase ywfH	122	3
28	P21882	Pyruvate dehydrogenase E1 comp. subunit beta	119	3
29	P80239	Alkyl hydroperoxide reductase subunit C	118	3
30	O31632	YjcJ protein	103	3

†MASCOT protein score based only on azhal-containing peptides, at least 2 peptides per protein

presence of azhal, although to a lesser extent than in the absence of both methionine and azhal. This suggests that cells do sense the lack of methionine and turn on methionine biosynthesis even in the presence of the methionine analogue.

The growth on azhal, after a lag-time of approximately 1 hour, implies that *B. subtilis* incorporates azhal into cellular proteins. This was examined by extracting proteins from cells grown for 8 hours on the analogue and digesting the extracted proteins with trypsin. Following tryptic digestion azhal-containing peptides were enriched and analyzed by mass spectrometry as described in detail in *Chapter 3*. Following isolation and mass spectrometric analysis, 626 unique peptides were identified of which 223 were found to contain azhal. These azhal-containing peptides were derived from 103 different proteins of which 54 were identified by two or more azhal-containing peptides (Table I).

TABLE I
continued

No.	Acc. No.	Description	Score†	No. Matches
31	P39126	Isocitrate dehydrogenase [NADP]	101	3
32	P09339	Aconitate hydratase	138	2
33	O31629	UPF0477 protein yjcG	129	2
34	P80868	Elongation factor G	118	2
35	P31104	Chorismate synthase	113	2
36	P13243	Probable fructose-bisphosphate aldolase	111	2
37	P04969	30S ribosomal protein S11	104	2
38	P49786	Biotin carboxyl car. prot. of ac.-CoA carboxylase	104	2
39	P02394	50S ribosomal protein L7/L12	101	2
40	O34660	Aldehyde dehydrogenase	96	2
41	P55873	50S ribosomal protein L20	89	2
42	P37808	ATP synthase subunit alpha	85	2
43	P06224	RNA polymerase sigma factor rpoD	82	2
44	O32157	YurP protein	82	2
45	P21471	30S ribosomal protein S10	81	2
46	P28015	Putative septation protein spoVG	79	2
47	O34934	Prob. inorg. polyphosphate/ATP-NAD kinase 2	77	2
48	O32174	Glycine cleavage system H protein	75	2
49	P08838	Phosphoenolpyruvate-protein phosphotransferase	75	2
50	P80643	Acyl carrier protein	69	2
51	P18255	Threonyl-tRNA synthetase 1	68	2
52	P80698	Trigger factor	65	2
53	Q06797	50S ribosomal protein L1	64	2
54	P80859	6-phosphogluconate dehydrog, decarboxylating 2	58	2

†MASCOT protein score based only on azhal-containing peptides, at least 2 peptides per protein

Incorporation of azhal into LacZ and effects on protein function— B. subtilis incorporates azhal into proteins as shown above. Indeed, the LacZ expression of cells grown on azhal suggested that methionine biosynthesis was not induced to the same extent as under full methionine starvation conditions without azhal. However, for the LacZ activity measurements of *B. subtilis* BR151 grown with azhal to be a reliable indication of *yitJ* expression, enzymatic activity of LacZ containing azhal should be comparable to activity of LacZ containing methionine. As the fusion gene used in *B. subtilis* stems from *E. coli*, the induction of the lac-operon in *E. coli* was tested in the presence of azhal. Cells grown on M9 minimal medium containing 19 amino acids were shifted to lactose-containing medium containing either methionine, azhal or neither as a negative control for three hours. Subsequently cells were

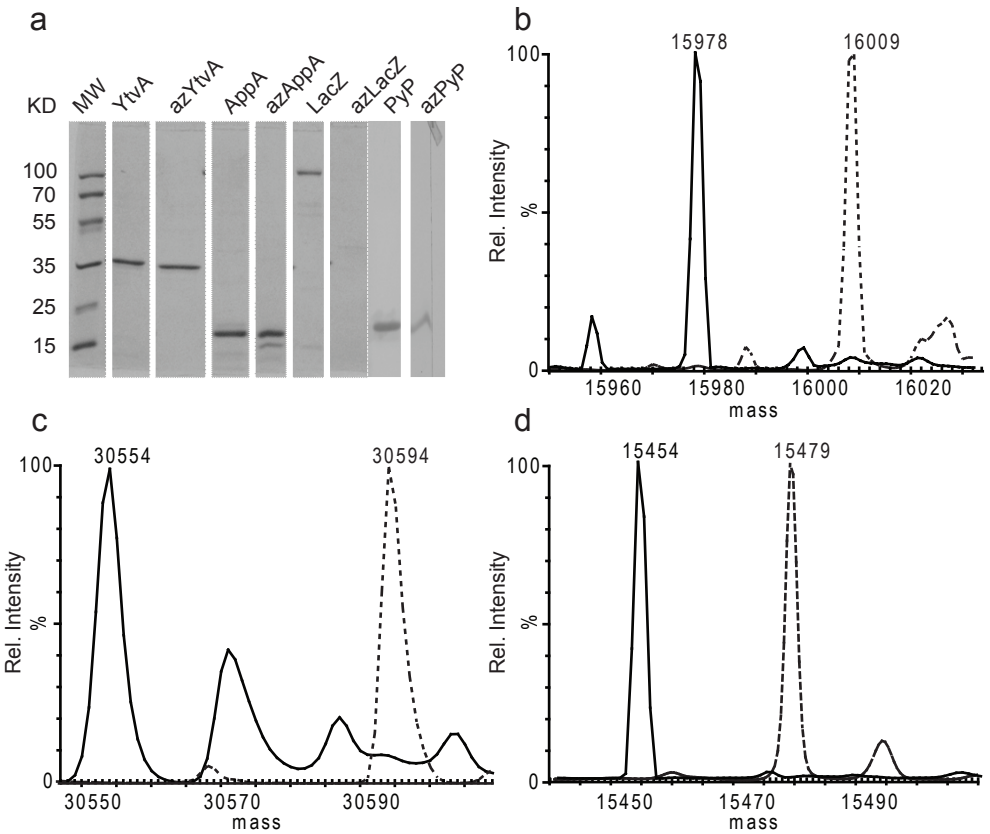

FIGURE 7. **Incorporation of azhal into recombinant proteins produced in *E. coli*.** SDS-PAGE gel after Ni-column purification of His-tagged recombinant proteins produced in *E. coli* grown in minimal medium containing either methionine or azhal (**a**). Overlay of deconvoluted-mass spectra of PYP (dotted line) and azPYP (solid line), theoretical mass of His-tagged PYP and its chromophore *p*-coumaric acid attached is 16007 Da (**b**). The mass difference of -31 amu shows that all six methionine residues have been replaced by azhal (mass difference azhal and methionine is -5 amu). Overlay of deconvoluted-mass spectra of YtvA (theoretical mass: 30593 Da) and azYtvA (**c**). The mass difference of -40 amu shows all eight methionine residues were replaced. Overlay of deconvoluted-mass spectra of $AppA_{5\text{-}125}$ (theoretical mass: 15479 Da) and $azAppA_{5\text{-}125}$ (**d**). The mass difference of -25 amu indicates that all 5 methionine residues have been replaced by azhal.

disrupted and assayed for LacZ activity. Clearly, cells in which the lac-operon is induced in the presence of azhal have LacZ activity comparable to that of the negative control, whereas cells grown in methionine containing medium show high LacZ activity (Figure 6b). To exclude that lactose import through the lactase transporter (LacY) prevents full induction of the operon, e.g. azhal-containing LacY may not import lactose efficiently, cells were also induced by the lactose analogue isopropyl β-D-1-thiogalactopyranoside (IPTG), not requiring a transporter for membrane passage (Figure 6b). Again cells grown on azhal did not show more induction of LacZ-activity than the negative control upon induction by IPTG. These results indicate that LacZ containing azhal has no, or a severely reduced, enzymatic activity.

To test whether azhal incorporation into LacZ leads to a markedly less functional protein we transformed *E. coli* with a pBAD plasmid containing LacZ under an arabinose-inducible promotor and a His-tag which enables purification for in vitro assays. Induction of LacZ production with arabinose again showed that cells grown in azhal-supplemented medium had the same level of LacZ activity as the negative control, whereas cells grown on methionine containing medium showed high levels of LacZ activity (Figure 6b). However, when LacZ was purified from the soluble protein fraction by Ni-affinity columns, no azhal-containing LacZ was recovered whereas large amounts of methionine containing LacZ could be purified (Figure 7a). This suggests that azhal-containing LacZ probably does not assemble correctly and precipitates into inclusion bodies and/or is rapidly degraded. Therefore, LacZ is not a suitable reporter to measure azhal induced activation of methionine biosynthesis in *B. subtilis.*

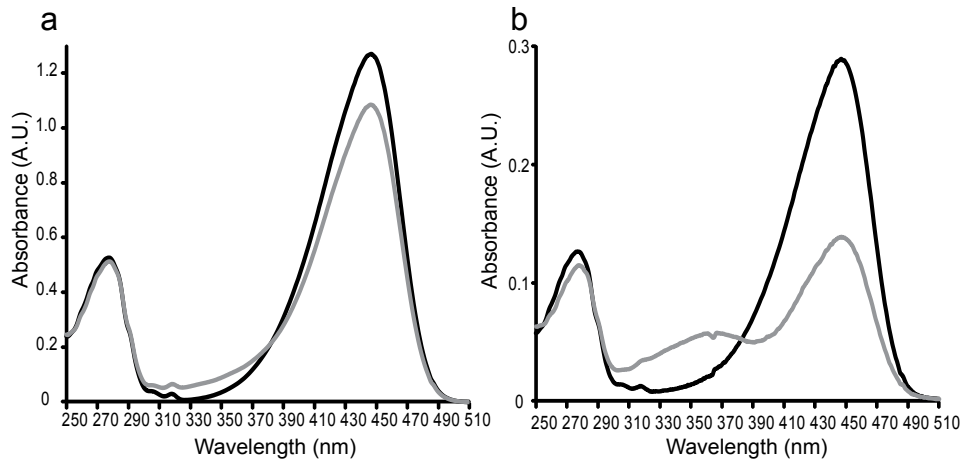

FIGURE 8. **UV-VIS Spectra of PYP and azPYP.** Spectrum of ground state (black line) and light activated state (grey line) after photoflash excitation of PYP (**a**) or azPYP (**b**). Ground state spectra of both PYP and azPYP are highly similar with absorbance maxima at 280 and 446 nm. Both have a marked reduction in absorbance at 446 nm and a blue shift to ~355 nm upon photoflash excitation, showing azPYP to be photo-active, with the same iso-bestic point at 383 nm.

Incorporation of azhal into photo-active proteins, effects on spectral properties and photocycle kinetics— To further study the effects of azhal incorporation on protein structure and function, we also produced three photo-active proteins in *E. coli* in the presence of azhal, under an IPTG inducible promotor. The three photo-active proteins are PYP (*H. halophila*), YtvA (*B. subtilis*) and the N-terminal BLUF domain of AppA (*Rb. sphaeroïdes*). Induction of expression in azhal-containing medium followed by reconstitution with their respective chromophores and Ni-column purification yielded three proteins (Figure 7a). Measured by their average mass shift compared to their methionine containing counterparts these proteins had all their methionine residues replaced by azhal (Figure 7b, c, d). This clearly demonstrates that methionine-auxotrophic *E. coli* incorporate azhal into proteins when grown in the presence of the methionine-analogue, and that these azhal-containing proteins are not all rapidly degraded or precipitate as seems to occur with LacZ.

To ascertain whether changing the methionine residues to azhal influences azPYP's structure around its chromophore, *p*-coumaric acid, the UV-VIS spectra of PYP and azPYP are compared in Figure 8. As is apparent from the ground state spectra, absorption maxima have not changed. Moreover, both proteins are photo-active and show bleaching at 446 nm and a blue shift to ~355 nm (pB) after excitation of the protein solution by photoflash illumination (Figure 1a). Subsequently, the recovery to the ground state was measured by determining the rate of recovery of absorbance at 446 nm upon photoflash excitation. Figure 9 and Table II show that the rate of recovery of azPYP (0.89 s^{-1}) is slightly lower than the rate of recovery measured for methionine containing PYP (1.28 s^{-1}). The rate measured for methionine containing PYP is somewhat less than the 2.0 s^{-1} to 3.4 s^{-1} reported in literature

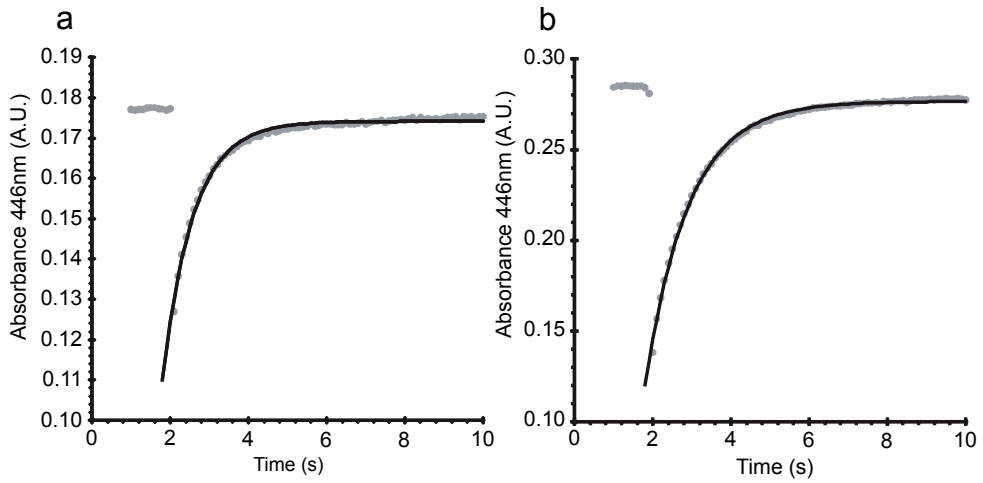

FIGURE 9. **Recovery of the absorbance at 446 nm of PYP and azPYP.** Figure shows the recovery of absorbance at 446 nm after photoflash excitation of PYP (**a**) and azPYP (**b**), grey dots are absorbance values measured before and after the excitation of the protein (at the 2 second time point), the black line is the fit of the mono-exponential function by Excel least squares analysis to the absorbance data. The recovery rates of these fits are presented in Table II.

(187-189). This could be due to differences in the purification procedure. Proteins in this study were only enriched on a Ni-column, yielding two variants with respect to the rate of recovery to the ground state (M.A. van der Horst, personal communication). Further purification can separate the slower recovering variant from the fast recovering one, resulting in a higher overall recovery rate. Furthermore proteins in this study did not have their histidine-tags removed, which also influences recovery rate. The methionine residue at position 100 plays an important role PYP photocycle kinetics through interaction with Arg_{52}, acting in stabilizing the ground state and facilitating the recovery from pB to the ground state after photo-activation (190, 191). Thus, as expected, mutants of M_{100} show a significantly slower recovery to ground state varying from $6.5*10^{-2}$ s^{-1} ($M_{100}E$) to $1.9*10^{-3}$ s^{-1} ($M_{100}L$ and $M_{100}A$) and $1.1*10^{-3}$ s^{-1} ($M_{100}K$) (190, 191). In comparison, replacement of all methionine residues including Met_{100} by azhal only marginally decreases the recovery rate to ground state.

TABLE II
Rate of recovery to ground-state after illumination of photo-active proteins

Protein	$\tau_{recovery}$ (s)	k (s^{-1})	$k_{rel.}$†	λ(nm)
PYP	0.78	1.28	1	446
azPYP	1.12	8.90×10^{-1}	0.69	446
AppA	600	1.67×10^{-3}	1	495
azAppA	175	5.73×10^{-3}	3.44	495
YtvA	3783	2.64×10^{-4}	1	450
azYtvA	4943	2.02×10^{-4}	0.77	450

† recovery rate relative to rate of methionine containing photo-active protein.

The chromophore (coumaric acid) is thought to be in anionic form in the active site and to be protonated during formation of the pB intermediate of the photocycle (192). The protonation state of the chromophore can be influenced by the pH. Lowering the pH results in reversible formation of a blue shifted intermediate at low pH called pB_{dark} (177, 192). Protonation of the chromophore is a cooperative process, presumably because of the existence of an extensive hydrogen-bonding network in the pG state which has to be disrupted (193). The formation of pB_{dark} was measured for azPYP by pH titration (Figure 10a) and the pK_a and Hill coefficient (*n*), which expresses the degree of cooperativity of the protonation were obtained (Figure 10b) and compared to PYP. The Hill coeffient (*n*) of azPYP (*n* =1.8) was the same as for PYP (*n* =1.8) which was consistent with earlier observations (192, 193) of methionine containing PYP. Azhal does not seem to influence the cooperativity of protonation

of the chromophore. However the pK_a of azPYP, (3.2) was slightly higher than the pK_a (2.8) for methionine containing PYP (177, 192, 193). As the pB and pB_{dark} intermediates result from partial unfolding of the protein (192), the slightly higher pKa of azPYP could indicate a somewhat less stable protein structure in azPYP compared to wild type PYP. All in all, azPYP appears to be functionally highly similar to wild type PYP with only slight alterations in photocycle recovery rate and protein stability

The effects of azhal incorporation on spectral properties of YtvA are shown in Figure 11. As for PYP, the ground state spectrum of azYtvA is highly similar to that of methionine containing YtvA. This shows that no major changes in structure occur that interfere with chromophore binding. After illumination, the azYtvA spectrum shifts to the same single maximum absorption at 386 nm as YtvA, confirming that azYtvA is photo-active too. The kinetics of recovery from illuminated to dark state of azYtvA are shown in Table II. The recovery rate of azYtvA ($2.02*10^{-4}$ s^{-1}) is only marginally slower than that of YtvA ($2.64*10^{-4}$ s^{-1}), which shows that replacing methionine residues with azhal does not have a large effect on YtvA's photocycle kinetics.

The spectrum of the BLUF-domain of AppA ($AppA_{5-125}$) produced in *E. coli* grown in azhal-containing medium also is very similar to its methionine containing counterpart (Figure 12). $azAppA_{5-125}$ was photo-active and showed the same ~10 nm red shift upon illumination. However, after illumination the rate of $azAppA_{5-125}$ recovery to the ground state was 3.4 fold faster than that of wild type $AppA_{5-125}$ (Table II). This surprising increase in recovery rate is reminiscent of the increase in recovery rate found for AppA $W_{104}F$ which is 2.7 fold that of wild type (194). Although $azAppA_{5-125}$ does not show a change in the red-shift after illumination, which is the case for the $W_{104}F$ mutant, the increased recovery could also indicate a destabilization of the signalling state (194) by azhal incorporation. In the BLUF-

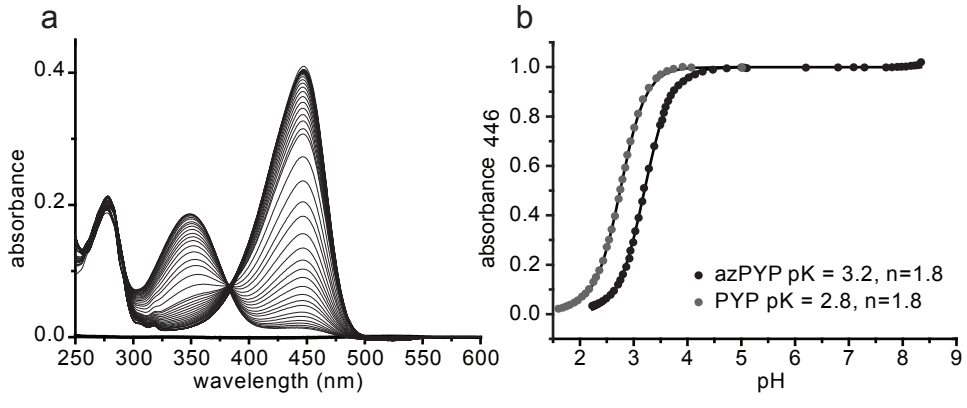

FIGURE 10. **pH titration of the absorption spectra of PYP and azPYP.** Dependence of the absorption spectra of azPYP on pH (**a**). Spectra were taken at room temperature between pH 1 and pH 8.5 at room temperature in 10 mM tris-Cl, 100 mM KCl. The relative amplitude of the absorbance at 446 nm as a function of pH for PYP (grey dots) and azPYP (black dots) (**b**). Theoretical curves (solid lines) were obtained by fitting the data to the modified Henderson Hasselbalch equation [1].

domain protein AppA the methionine at position 106, conserved in other BLUF-domain proteins, is thought to change its interaction with Glu_{63} during light induced conformational changes in the protein (195-197). Although all methionine residues were replaced by azhal, the altered kinetics of the rate of recovery to the ground state does support the notion of the involvement of this specific methionine residue in the conformational changes of the protein in ways that cannot be exactly mimicked by the methionine analogue azhal.

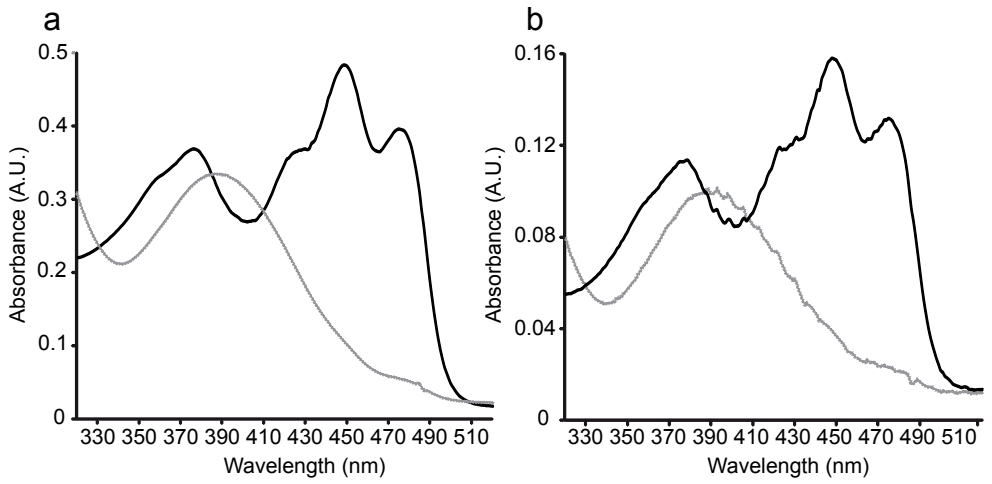

Figure 11. **UV-VIS Spectra of YtvA and azYtvA.** Spectrum of dark state (black line) and illuminated state (grey line) after illumination of YtvA (**a**) and azYtvA (**b**). Ground-state spectra of YtvA and azYtvA are similar with maxima of absorbance at 376, 448 and 475 nm. Just like YtvA, azYtvA shows photo-activity and the illuminated state shows the same single maximum at 386 nm, with iso-bestic points observed at 331, 386 and 409 nm.

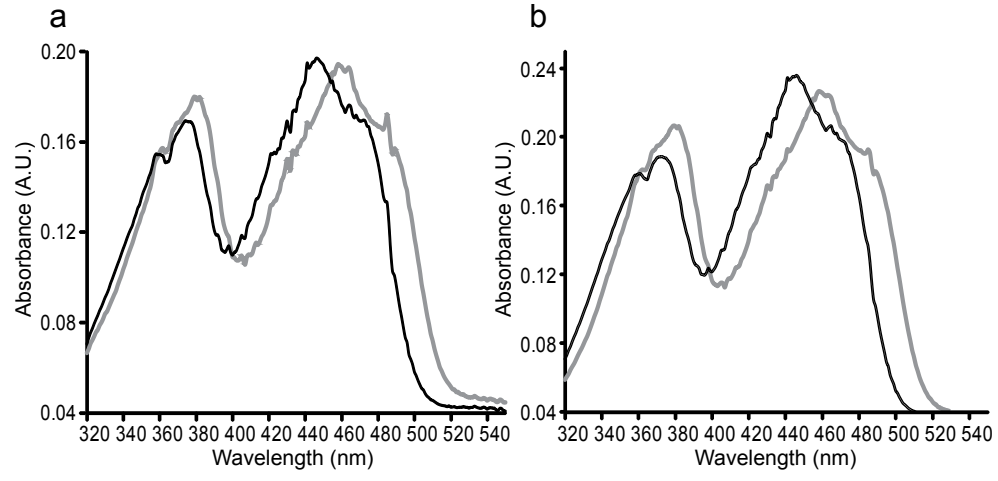

Figure 12. **UV-VIS Spectra of $AppA_{5-125}$ and $azAppA_{5-125}$.** Spectrum of dark state (black line) and illuminated state (grey line) after illumination of $AppA_{5-125}$ (**a**) and $azAppA_{5-125}$ (**b**). Ground-state spectra of $AppA_{5-125}$ and $azAppA_{5-125}$ are very similar, exhibiting major absorbance maxima at 374 and 446 nm. $azAppA_{5-125}$ is photo-active and also shows a red shift ~10 nm to an illuminated state with maxima at 380 and 460 nm, like $AppA_{5-125}$. Both proteins exhibit iso-bestic points at 359, 398 and 454 nm.

Discussion

Azhal's suitability for pulse-labelling was tested by measuring growth and viability of *E. coli* grown on a medium with azhal substituting for methionine. Growth rate, viability and cellular protein content were comparable for cells grown on azhal or methionine for the initial 30 minutes. Free azhal, not incorporated into proteins, gave no evidence of toxicity, since an excess of azhal in the presence of saturating amounts of methionine has no effect on growth rate. After prolonged labelling however, growth arrest does occur, which can be explained by dysfunction of essential proteins with crucial roles for one or more methionine residues. Another possible explanation for the occurrence of growth arrest is the role of methionine as a methyl donor for methylation reactions in the form of s-adenosyl methionine. As is obvious from its structure azhal cannot replace methionine in this function and as such would cause methylation signalling to go awry, possibly causing growth arrest. Nevertheless, because initial growth rate and protein formation seem unaffected, azhal seems a promising label for short time-scale proteome-wide pulse-labelling studies in *E. coli*.

In stark contrast to *E. coli,* growth of *B. subtilis* on azhal at 200 mg/l showed a prolonged lag phase, and growth was less than 3 fold slower. In addition *B. subtilis* did not go into stationary phase in the time-scale measured. Concentrations of 800 mg/l did induce complete growth arrest. Strikingly, no effect on initial growth rate of *E. coli* was observed at this azhal concentration both in the absence and presence of methionine. With *B. subtilis,* mixtures of methionine and azhal gave an initial lag phase and diminished growth rate. This suggests a secondary toxic effect independent of incorporation into cellular proteins, consistent with the absence of growth at higher azhal concentrations. In spite of the observation that *B. subtilis* incorporates azhal into cellular protein, both the different growth on azhal, the suspected secondary toxicity and in particular the initial lag phase, lead to the conclusion that azhal is not the most suitable label for pulse-labelling experiments in *B. subtilis*. This result is surprising as in addition to *E. coli*, growth on azhal has been reported for various eukaryotes (141, 143, 144, 148, 169, 171). In contrast however, we previously found that *Saccharomyces cerevisiae* also showed growth inhibition that was dependent on the concentration of azhal in the medium (Supplemental Figure 1). This shows that although azhal-labelling seems applicable to a variety of organisms, labelling and growth needs to be tested for each prospective organism.

Suitability of an amino acid analogue for pulse-labelling requires that incorporation in proteins should have no important effect on protein folding and stability. The highly different physiological responses of two bacteria growing on the methionine analogue azhal, sparks the question about how incorporation of the analogue affects protein structure and function. This was tested by production of various recombinant proteins in *E. coli* grown in the presence of azhal. In line with earlier reports (143, 144, 148, 176) we observed that *E. coli* readily incorporated the analogue into PYP, YtvA and AppA. Judged from their ground-state UV-VIS spectra these proteins folded normally and retained photo-activity upon illumination. Measurements on the rate of recovery from signalling to ground state for these

proteins showed a slight decrease in recovery rate for azPYP and azYtvA, i.e. these proteins remain in the signalling state somewhat longer. In contrast, the recovery rate of azAppA increased significantly, suggesting strong destabilization of the signalling state. pH-titration experiments with azPYP also suggested a slightly destabilized ground-state structure. However, on the whole the three proteins kept their activity and were correctly folded as observed before with other proteins and protein complexes (144, 148, 151, 176). In sharp contrast to these findings, LacZ activity was not measurable when induced in cells grown in azhal-containing medium and His-tagged azLacZ could not be purified from the soluble protein fraction of *E. coli*. This strongly suggest misfolding and precipitation or accelerated degradation of azhal-containing LacZ.

Though similar in electron density to methionine (144), azhal cannot substitute methionine for all its physio-chemical characteristics in a cellular context as illustrated by the non-functional azLacZ protein. The misfolding and subsequent degradation of a subset of proteins is a possible cause of the eventual growth arrest in *E. coli* after 30 minutes and in proteome-wide pulse experiments these proteins will probably escape detection. However, both the initial growth rate of *E. coli* on azhal and minor effects of azhal incorporation on the structure and function of proteins described here and in literature (148, 150, 151, 176) suggest that it can give an accurate measure of cellular translation rates for most proteins.

Supplemental Data—Supplemental figures and tables can be found in the addendum section on page 134.

Experimental Procedures

Synthesis of L-azhal— L-azhal was synthesized from L-Boc-2,4-di-aminobutyric acid (L-Boc-DAB, Chem-Impex, Wood Dale, USA) by diazotransfer (198) using Triflic azide (TfN_3) as previously described (141).

Strains and plasmids— Chemically competent CAG18491 cells (*E. coli* genetic stock centre Yale, USA) were transformed with pREP4 (Qiagen, Venlo, the Netherlands) to make CAG18491/pREP4. Subsequently, chemically competent CAG18491/pREP4 were transformed with plasmids pHISP (199), pQE30X$_a$/AppA$_{5\text{-}125}$ (200), pQE30X$_a$/YtvA (201) or pBAD/His/LacZ (Invitrogen, Breda, the Netherlands) to generate the protein production strains (Table III).

Cell culture, growth curves, viability- and β-galactosidase assays— *E. coli* strain MTD123 (180) was grown aerobically at 37 °C in LB medium. For growth experiments cells grown overnight in LB medium were transferred to M9 minimal medium containing 6.8 µM $CaCl_2$, 1.0 mM $MgSO_4$, 59.3 µM thiamine·HCl, 57.0 nM Na_2SeO_3, 5.0 µM $CuCl_2$, 10.0 µM CoCl, 5.2 µM H_3BO_3, 99.9 µM $FeCl_3$, 50.5 µM $MnCl_2$, 25.3 µM ZnO, 0.08 µM Na_4MoO_4, 111 mM glucose with 40 mg/l of tyrosine and 60 mg/l of each of the other 19 natural amino acids (Sigma-Aldrich, St Louis, USA). Cells were inoculated at OD_{600} 0.1 and allowed to grow into exponential phase before being harvested at OD_{600} 1.0, by spinning down the cells for 10 minutes at 4500 rpm and 4 °C. Cells were then washed twice by resuspending the cell pellet in sterile M9 medium without additives (followed by centrifugation) to eliminate traces of methionine. After washing, cells were transferred to M9 minimal medium (see above) in which the methionine was replaced by azhal and cells were allowed to resume growth aerobically at 37 °C. Growth curves were recorded with varying methionine or azhal conditions as indicated.

To determine the number of viable cells, cells were diluted in sterile M9 medium and plated on LB-

agar plates in duplo; colonies were counted after overnight growth at 37 °C. β-Galactosidase assays were performed essentially as described by Miller (202). In short, cells (CAG18491/LacZ) were induced with lactose (2% final concentration), IPTG (200 µM final concentration) or arabinose (1% final concentration) for 3 hours. Next, cells were disrupted by the addition of 0.1% SDS, 1% chloroform and placed on ice. Subsequently 1 mM ortho-nitrophenyl-β-galactoside was added and the reaction was allowed to proceed at 37 °C until being stopped by the addition of 1 M Na_2CO_3 to the reactions. B-galactosidase activity was measured at 420 nm and corrected for reaction volume, OD_{600} and reaction time to yield Miller units.

The *B. subtilis* strain BR151 (auxotrophic for met, arg, lys) was grown aerobically at 37 °C in Spizizen minimal medium (203) with addition of 50 mg/l methionine, arginine and lysine. Cells were allowed to grow into early exponential phase before being harvested, and washed twice with minimal medium at room temperature. After washing, cells were transferred to minimal medium (see above) in which methionine was replaced by azhal and cells were allowed to resume growth aerobically at 37 °C. Growth curves were recorded using a Klett-Summerson photoelectric colorimeter with methionine or azhal conditions as indicated. B-galactosidase assays were performed as described above.

TABLE III
E. coli and B. subtilis strains and plasmids used in this study

name	organism	genotype	plasmids	resistance	source
MTD123	*E. coli*	ΔyagD, ΔmetE, ΔmetH	-	-	(180)
CAG18491	*E. coli*	λ^-, rph-1, metEo-3079::Tn10	-	tet	(206, 207)
CAG18491/pRep4	*E. coli*	λ^-, rph-1, metEo-3079::Tn10	pREP4	kan, tet	this study
CAG18491/PYP	*E. coli*	λ^-, rph-1, metEo-3079::Tn10	pREP4, pHISP	amp, kan, tet	this study
CAG18491/APPA	*E. coli*	λ^-, rph-1, metEo-3079::Tn10	pREP4, pQE30X$_a$/APPA$_{5-125}$	amp, kan, tet	this study
CAG18491/YTVA	*E. coli*	λ^-, rph-1, metEo-3079::Tn10	pREP4, pQE30X$_a$/YTVA	amp, kan, tet	this study
CAG18491/LacZ	*E. coli*	λ^-, rph-1, metEo-3079::Tn10	pREP4, pBAD/His/LacZ	amp, kan, tet	this study
M15MA	*E. coli*	Na^{IS}, Str^S, Rif^S, Thi$^-$, Lac$^-$, Ara$^+$, Gal$^+$, Mtl$^-$, F$^-$, RecA$^+$, Uvr$^+$, Lon$^+$. metEo	pREP4	kan	(148)
BR151:*yitJ-lacZ*	*B. subtilis*	trpC2, metB10, lys-3, *yitJ-lacZ*	-	-	(208)

Production and purification of recombinant proteins containing azhal— Cells were grown into early exponential phase at 37 °C in 500 ml M9 minimal medium as described above, adding 60 mg/l methionine, 50 µg/l tetracycline, 50 µg/l ampicillin and 50 µg/l kanamycin. For production of YtvA, cells were grown in the dark and the protein was protected from light throughout the purification procedure and before subsequent measurements. Cells were induced directly in the methionine containing medium with 100 µm IPTG (PYP, AppA, YtvA) or 1% arabinose (LacZ) before a further 3 hours of incubation in a shaking incubator set at 37 °C. Alternatively, cells were harvested, washed twice with M9 buffer, inoculated in 500 ml minimal medium with antibiotics but lacking methionine and incubated at 37 °C for half an hour before addition of 400 mg/l azhal prior to induction. Cells were subsequently harvested

by centrifugation, resuspended in 100 mM tris-Cl pH 8.0, 1 mg/ml lysozyme, 25µg/ml DNase/RNase and lysed by sonication. Lysates were centrifuged at 15000 rpm for 45 minutes at 4 °C to remove cellular debris. Subsequently, photo-active proteins were reconstituted with their respective chromophores as described below before they were loaded on a Ni-agarose column (Qiagen, Venlo, the Netherlands) by gravity flow. Columns were washed with 50 ml 100 mM tris-Cl pH 8.0 before samples were eluted with 8 ml 500 mM imidazole in 100 mM tris-Cl pH 8.0 and dialyzed immediately against 100 mM tris-Cl pH 8.0 in 5kD cut-off dialysis tubing (Spectrum Laboratories, Rancho Dominguez, USA) overnight at 4 °C.

Reconstitution of chromophores in photoproteins— Prior to purification, photo-active proteins were reconstituted with their respective chromophores to yield photo-active holo-proteins. PYP was incubated with an activated-ester form of *p*-coumaric acid for an hour at room temperature in the dark (204). Cell free extract containing AppA was incubated with an excess of flavin adenine dinucleotide (>95% pure, Sigma-Aldrich) while YtvA was incubated with an excess of riboflavin 5′ monophosphate (>85% pure, Sigma-Aldrich), both for an hour on ice in the dark.

UV-VIS Spectroscopy— Measurement of absorbance spectra and photocycle kinetics were performed on a HP 8453 diode array spectrophotometer (Hewlett Packard). Kinetic measurements were taken with a time resolution of 100 ms after white light photoflash excitation of PYP in 100 mM tris-Cl (pH 8.0). For measurement of the rate of receptor state recovery, AppA and YtvA (in 100 mM tris–Cl, pH 8.0) were irradiated with saturating actinic white light from a Schott KL1500 light source and allowed to revert to the receptor state in the dark. Spectra were recorded every 30 s for 45 minutes (AppA) or every 60 seconds for 120 minutes (YtvA). Absorption changes at 450 nm (YtvA) and 495 nm (AppA) were analyzed by mono-exponential fits to the data using the solver function of Excel (Microsoft corporation, Redmond, USA) in least squares analysis as described before (205). Absorption changes at 446 nm for PYP were analyzed by both mono- and bi-exponential fits to the data to account for the contribution of a slower recovering variant of the protein. However because bi-exponential fits did not yield different or better fitting results, mono-exponential fits to the data are also presented for PYP.

pH-titrations of PYP and azPYP— pH titrations were carried out according to Hoff *et al.* (192) in 10 mM tris-Cl, 100 mM KCl buffer. pK_a values, and *n*-values (or: Hill coefficients) expressing the degree of cooperativity, were calculated by fitting the data to a modified Henderson-Hasselbalch equation [1], in which *n* describes the steepness of the transition by using the solver function of Excel in least squares analysis as described above.

$$pG = \frac{1}{1+10^{n(pH-pK)}} \qquad [1]$$

Sample preparation for Mass spectrometry— For holo-mass measurements proteins were desalted on a C_4 (YtvA) or C_{18} (PYP, AppA) Ziptip (Millipore, Bedford, USA), and eluted in 60% acetonitrile, 0.1% formic acid, 49.9% water prior to mass analysis. For peptide mass fingerprinting and tandem-MS experiments, proteins were digested overnight with 1:50 (w/w) protease:protein, with trypsin gold mass spectrometry grade (Promega, Madison, USA) at 37 °C. Prior to analysis, peptides were desalted with Ziptip C_{18} (Millipore, Bedfort, USA) and eluted in 60% acetonitrile, 0.1% TFA, 49.9% water and diluted 10 times before being loaded on the reversed phase chromatography system. *B. subtilis* lysates were obtained by sonication as described above and were digested overnight with trypsin gold mass spectrometry grade, before azhal peptides were enriched by diagonal chromatography as described in *Chapter 3*. Subsequently, enriched pools were loaded on the LC tandem-MS system described below.

Mass spectrometry— Reflectron MALDI-TOF mass spectra were recorded on a Micromass TofSpec 2EC (Micromass, Whyttenshawe, UK). Holo-masses of proteins were determined by offline spray using Econo12 coated-glass emitters (New objective, Woburn, USA) and a quadrupole time-of-flight mass spectrometer (Q-TOF; Micromass, Waters, Manchester, UK). Samples for LC tandem-MS studies were separated on a reversed phase capillary column (150 mm x 75-µm PepMap C_{18}; LC Packings, Amsterdam, The Netherlands). Sample introduction

and mobile phase delivery at 300 nl/min. were performed using a Ultimate nano-LC-system (Dionex, Sunnyvale, CA) equipped with a 10-µl injection loop. All solvents used are of LC-MS grade (Biosolve, Valkenswaard, the Netherlands). Mobile phase A was water + 0.1% formic acid, and mobile phase B was 50% acetonitrile, 50% water + 0.1% formic acid. For separation of peptides, a two step gradient of 5 – 100% solvent B over 22 minutes was used. Eluting peptides were electrosprayed into a Q-TOF (Waters, Manchester, UK). The most abundant ions from the survey spectrum, ranging from m/z 350 to 1500, were automatically selected for collision-induced fragmentation using Masslynx (Waters, Manchester, UK). Fragmentation was conducted with argon as collision gas at a pressure of 4 x 10^{-5} bars measured on the quadrupole pressure gauge.

Data analysis— Mass spectra of intact proteins were smoothed (Masslynx using a Savitsky-Golay smoothing filter with smoothing window and number of iterations set to 2) and deconvoluted (using the Maxent algorithm) to obtain average masses for the proteins measured. Deconvoluted peak lists from tandem-mass spectrometry experiments were generated by proteinlynx. Next, these pkl-files were combined using notepad. Combined pkl files were submitted to the the MASCOT search engine version 2.1 (Matrix Science, London, United Kingdom) using search parameters as described in detail in *Chapter 3* to identify azhal-containing peptides. A search with these parameters was conducted in a local database of the *B. subtilis* proteome (4238 sequences, 1269237 residues, release 14.2, October 1, 2008, Uniprot consortium). A significance threshold of 0.01 was set, resulting in a threshold score of 38. 'Mudpit scoring' and an ion score cut-off of 38 was applied in order to assure that all assigned peptides had a p-value of <0.01.